

Technology Development for Iron and Cobalt Fischer-Tropsch Catalysts

Quarterly Report

October 1, 2001 to December 31, 2001

Burtron H. Davis

Enrique Iglesia (UC/B Subcontract)

DE-FC26-98FT40308

University of Kentucky Research Foundation

201 Kinkead Hall

Lexington, KY 40506

University of California-Berkeley (Subcontract)

Laboratory for the Science and Application of Catalysis

Department of Chemical Engineering

University of California at Berkeley

Berkeley, CA 94720

Disclaimer

This report was prepared as an account of work sponsored by an agency of the United States Government. Neither the United States Government nor any agency thereof, nor any of their employees, makes any warranty, express or implied, or assumes any legal liability or responsibility for the accuracy, completeness, or usefulness of any information, apparatus, product, or process disclosed, or represents that its use would not infringe privately owned rights. Reference herein to any specific commercial product, process, or service by trade name, trademark, manufacturer, or otherwise does not necessarily constitute or imply its endorsement, recommendation or favoring by the United States Government or any agency thereof. The views and opinions of authors expressed herein do not necessarily state or reflect those of the United States Government or any agency thereof.

Abstract

CAER

Tight control of catalyst distribution within SBCRs should be maintained in order to quantify activity decline, especially for small pilot plant systems. Transient problems with previous SBCR experiments were caused by a maldistribution of catalyst between the reactor and slurry filtration system. The level indication/control system installed in an enhanced SBCR was robust and effective in maintaining a steady inventory of catalyst slurry in contact with the gas-phase. Measured deactivation rates in the enhanced SBCR system were comparable to that of CSTR experiments under similar conditions.

Attrition tests in the SBCR system indicated that the most of the catalyst breakdown occurred during catalyst activation and the initial synthesis stage; however, further research will be required to investigate the possibility of particle size classification/segregation at the sampling points. After activation, the catalyst particle mean diameter decreased in an exponential decay fashion. Attrition effects must be considered in order to accurately estimate the space velocity in pilot-scale SBCRs.

A cobalt catalyst (25%Co/ γ -Al₂O₃, prepared by slurry phase impregnation) was used in a fixed bed reactor under a pressure/density tuned supercritical fluid mixture of n-pentane/n-hexane. By using an inert gas as a balancing gas to maintain a constant pressure, the density of the supercritical fluid could be tuned near the supercritical point while maintaining constant space velocity within the reactor. The benefits of the mixture allowed for optimization of transport and solubility properties at an appropriate reaction temperature for Fischer Tropsch synthesis with a cobalt catalyst. There was an important increase in conversion due to greater accessibility to active sites after extraction of heavy wax from the catalyst, and additional

benefits included decreased methane and carbon dioxide selectivities. Decreased paraffin/(olefin + paraffin) selectivities with increasing carbon number were also observed, in line with extraction of the hydrocarbons from the pore. Removal of the wax products resulted in lower residence times in the catalyst pores and, therefore, decreased probability for readsorption and reaction to the hydrogenated product. Even so, there was not an increase in the alpha value over that obtained with just the inert gas.

Table of Contents

	<u>Page</u>
Disclaimer	1
Abstract	2
Table of Contents	4
Executive Summary	5
Task 1. Iron Catalyst Preparation	7
Task 2. Catalyst Testing	7
A. Slurry Bubble Activities	7
Task 3. Catalyst Characterization	20
Task 4. Wax/Catalyst Separation	20
Task 5. Oxygenates	20
Task 6. Literature Review of Prior Fischer-Tropsch Synthesis with Co Catalysts	20
Task 7. Co Catalyst Preparation	20
Task 8. Co Catalyst Testing for Activity and Kinetic Rate Correlations	21
A. Fischer-Tropsch Synthesis: Supercritical Conversion Using a Co/Al ₂ O ₃ Catalyst in a Fixed Bed Reactor	21
Task 9. Co Catalyst Life Testing	77
Task 10. Co Catalyst Mechanism Study	77
Task 11. University of California, Berkeley (Subcontract)	77
Task 12. Reporting and Management	77

Executive Summary

CAER

A Slurry Bubble Column Reactor (SBCR) is a gas-liquid-solid reactor in which the finely divided solid catalyst is suspended in the liquid by rising gas bubbles. The synthesis gas flows in a bubble phase through the catalyst/wax suspension. A gas distributor located in the bottom of the reactor produces the bubbles that rise inside the reactor. The volatile products are removed overhead together with unconverted gases, and the liquid products are separated from the catalyst suspension through a filter.

A considerable interest has been expressed in using SBCRs to carry out Fischer-Tropsch Synthesis (FTS), particularly for the conversion of stranded natural gas into liquids. Historically, wall effects in small-scale SBCR reactors (diameters less than 30 cm) have presented many challenges with regard to interpretation of kinetic/conversion data for process scale-up. In this paper, we describe a novel 5-cm diameter SBCR system that incorporates a natural slurry recirculation loop that minimizes wall effects and promotes plug-flow behavior in the liquid phase. Conversion performance, catalyst activity decline, and attrition of a precipitated Fe/K FTS catalyst in the improved SBCR is compared to that of a CSTR run using the same catalyst and operating conditions.

Slurry back-mixing in the improved SBCR was significantly reduced by the addition of the down-comer/dip-tube flow path; consequently, the gas and liquid phases likely exhibited more plug-flow behavior. Thus, for a given space velocity, the enhanced SBCR yielded a higher conversion than that of the CSTR. The activity decline measured in the revamped SBCR system was shown to be similar to that of the CSTR experiments. Attrition tests in the SBCR system indicated that the most of the catalyst breakdown occurred between the time period of loading and activation; however, further research will be required to investigate the possibility of particle

size classification/segregation at the sampling points. After activation, the catalyst particle mean diameter decreased in an exponential decay fashion.

The anticipated benefits of running FTS in a supercritical fixed bed reactor are clear. In comparison with gas phase fixed bed processes, by using well pressure tuned supercritical media, in this case a C_5/C_6 mixture, the condensation of high molecular weight hydrocarbons leading to catalyst deactivation was avoided. In contrast to conventional slurry phase processes, which suffer from catalyst attrition, whereby the catalyst fines eventually breakdown to the point at which they can channel through the filter, running FTS under the supercritical media avoided this problem altogether. With the increase in conversion due to greater accessibility to active sites after wax extraction, additional benefits included decreased methane and carbon dioxide selectivities. The decreased paraffin/(olefin + paraffin) selectivities with increasing carbon number was in line with extraction of the hydrocarbon from the pore. Two possibilities are considered. Faster diffusion rates of wax products may result in lower residence times in the pores, and therefore, decreased probability for readsorption and reaction to the hydrogenated product. A more probable explanation is that the residence times of intermediate olefins, which are inversely related to their saturation vapor pressures, are decreased due to removal of the liquid phase during extraction.

Task 1. Iron Catalyst Preparation

The objective of this task is to produce robust intermediate- and high- α catalysts.

No scheduled or further activity to report.

Task 2. Catalyst Testing

The objective of this task is to obtain catalyst performance on the catalysts prepared in Task 1.

A. Slurry Bubble Activities

Executive Summary

A Slurry Bubble Column Reactor (SBCR) is a gas-liquid-solid reactor in which the finely divided solid catalyst is suspended in the liquid by rising gas bubbles. The synthesis gas flows in a bubble phase through the catalyst/wax suspension. A gas distributor located in the bottom of the reactor produces the bubbles that rise inside the reactor. The volatile products are removed over together with unconverted gases, and the liquid products are separated from the catalyst suspension through a filter.

A considerable interest has been expressed in using SBCRs to carry out Fischer-Tropsch Synthesis (FTS), particularly for the conversion of stranded natural gas into liquids. Historically, wall effects in small-scale SBCR reactors (diameters less than 30 cm) have presented many challenges with regard to interpretation of kinetic/conversion data for process scale-up. In this paper, we describe a novel 5-cm diameter SBCR system that incorporates a natural slurry recirculation loop that minimizes wall effects and promotes plug-flow behavior in the liquid phase. Conversion performance, catalyst activity decline, and attrition of a precipitated Fe/K FTS catalyst in the improved SBCR is compared to that of a CSTR run using the same catalyst and operating conditions.

Slurry back-mixing in the improved SBCR was significantly reduced by the addition of the down-comer/dip-tube flow path; consequently, the gas and liquid phases likely exhibited more plug-flow behavior. Thus, for a given space velocity, the enhanced SBCR yielded a higher conversion than that of the CSTR. The activity decline measured in the revamped SBCR system was shown to be similar to that of the CSTR experiments. Attrition tests in the SBCR system indicated that the most of the catalyst breakdown occurred between the time period of loading and activation; however, further research will be required to investigate the possibility of particle size classification/segregation at the sampling points. After activation, the catalyst particle mean diameter decreased in an exponential decay fashion.

Introduction

The Prototype Integrated Process Unit (PIPU) is a pilot plant system built in the early 1980s at the University of Kentucky for studying a multitude of synthetic fuel/chemical processes. Recently, a direct coal liquefaction reactor within the PIPU plant was reconfigured as a SBCR for FTS studies (see Figure 1.). The reactor was originally designed to operate with coarse catalyst pellets ($>500\ \mu\text{m}$). Consequently, the reactor system did not contain a wax separation system sufficient for smaller catalyst particles that are typically used in FTS. Therefore, a slurry accumulator and a batch wax filtration system were installed.

Early attempts to operate the pilot-scale reactor in a F-T mode were successful in that a clear wax product could be obtained. However, the initial activity observed in the bubble column was about 10-15% less than that of comparable CSTR runs. Also, the rate of conversion decline (and apparent catalyst deactivation) in the SBCR was much greater than that observed in the CSTR. It was hypothesized that the apparent increased deactivation rate in the SBCR was caused by the depletion of catalyst inventory due to the nature of the wax/catalyst separation system.

The CAER SBCR plant was overhauled and redesigned to incorporate automatic slurry level control and wax filtration systems. These design changes allowed for a more constant inventory of the catalyst to be maintained in the reactor while reducing slurry hold-up in the catalyst/wax separation system. In addition, the wax filtration system was rearranged to accept a variety of filter elements. These additions were meant to enhance the stability of the reactor operation so that long-term tests can be conducted to study catalyst deactivation and attrition under real-world conditions.

In the following discussion, we will detail the results and operational experiences of a catalyst attrition test with the enhanced SBCR system. Objectives of the study were to: Compare the performance of a precipitated Fe/K Fischer Tropsch Synthesis (FTS) catalyst in the enhanced SBCR and a continuous stirred tank reactor (CSTR); and Determine change of the catalyst distribution within the reactor system due to particle attrition effects.

Experimental

All FTS runs were conducted in either CSTR or SBCR systems. Activation and synthesis conditions for both reactor configurations are listed in Table 1. A precipitated iron catalyst having atomic composition of 100 Fe/4.4 Si/1K was used for this series of experiments.

Table 1. Operating Conditions for SBCR and CSTR Comparison Experiments.

	SBCR	CSTR
H ₂ /CO Ratio	0.7	0.7
Gas Space Velocity (SL/hr-g Fe)	5.0	5.15
Temperature (°C)	270	270
Pressure (Mpa)	1.21	1.21
Gas Superficial Velocity (cm/s)	3	750 RPM

CSTR Apparatus. The one-liter CSTR used in this study has been described in detail in the literature [1-2]. The following is a brief description of the reactor system.

The synthesis gas was delivered to the catalyst slurry via a sparger tube located below an impeller blade turning at 750 rpm. The reactor effluent exited the reactor and passed sequentially through two traps maintained at 333 and 273 K. Accumulated reactor wax was removed daily through a tube fitted with a porous metal filter. A dry flow meter was used to measure the exit gas flow rate.

SBCR Apparatus. A schematic of the SBCR apparatus is shown in Figure 1. In the current configuration, the bubble column has a 5.08 cm diameter and a 2 m height with an effective reactor volume of 3.7 liters. The synthesis gas was passed continuously through the reactor and distributed by a sparger near the bottom of the reactor vessel. The product gas and slurry exit the top of the reactor and pass through an overhead receiver vessel where the slurry was disengaged from the gas-phase. Vapor products and unreacted syngas exit the overhead vessel, enter a warm trap (333 K) followed by a cold trap (273 K). A dry flow meter downstream of the cold trap was used to measure the exit gas flow rate.

A dip tube was added to the reactor vessel so that the F-T catalyst slurry could be recycled internally via a natural convection loop. The unreacted syngas, F-T products, and slurry exited into a side port near the top of the reactor vessel and entered a riser tube. The driving force for the recirculation flow was essentially the difference in density between the fluid column in the riser (slurry and gas) and that of the dip-tube (slurry only). The dip tube provided a downward flow path for the slurry without interfering with the upward flow of the turbulent syngas slurry mixture. Thus, to some degree, back mixing of the slurry phase and wall effects in the narrow reactor [3] tube were minimized.

Based upon the analysis of the initial SBCR pilot plant runs, several more design changes were carried out to the system to increase the conversion stability. An automatic level controller was added to the overhead slurry/gas separation tank. This insured a constant inventory of

catalyst particles was being maintained in the reactor vessel if the superficial gas velocity within the column was constant.

Originally, the overhead separator vessel was designed to enhance settling of the catalyst particles. Thus, slurry to be filtered was extracted near the top of the vessel where the catalyst concentration would be lower than that near the bottom. Unfortunately, this approach required a large hold-up volume of slurry outside the reactor (greater than the reactor volume itself). Hold-up of slurry outside the reactor was lowered by decreasing the volume of the overhead vessel from 18 to 4 liters.

The sintered metal filter tube was moved to the liquid down comer below the overhead separation vessel. Currently, the filter is a flow-through device having a sintered metal tube in a shell. Filtered wax was extracted radially through the tube while slurry flows downward in the axial direction. The shear force of the axial slurry flow prevented excessive caking of the catalyst around the filter media. Filtered wax was metered into a storage tank through a let-down valve operated by the overhead liquid level controller. Pressure drop across the filter media can be varied manually by varying the wax storage tank pressure. The filter assembly was configured such that the filter media could be replaced on-line, without aborting or interrupting the reactor run.

The level or volume of the slurry within the receiver was continuously monitored by measuring the differential pressure across the height of the vessel. Argon was purged through each of the pressure legs to keep the lines free of slurry. Slurry volume within the receiver was controlled to be no more than 1.3 liters by removing wax from the reactor system via the level control valve. The unfiltered slurry flowed back to the reactor via a natural convection loop through a dip-tube exiting near the bottom of a reactor.

Samples of the unfiltered slurry were taken from the bottom of the reactor vessel and the overhead receiver tank on a daily basis. Wax products were Soxhlet extracted according to the method of McCartney [4]. The particle size distributions of the extracted catalyst particles were quantified using a light scattering technique by a Cilas 1064 liquid/particle analyzer.

Results and Discussion

SBCR Conversion Comparisons between CSTR and SBCR runs. One of the objectives of the run was to compare the performance of the enhanced SBCR with that of a CSTR configuration. It was anticipated that the modified SBCR system performance, in terms of catalyst deactivation, would be comparable to that of the CSTR experiments. The run/activation conditions for the enhanced SBCR system along with the comparison SBCR and CSTR conditions are listed in Table 1.

The CO gas conversions versus time-on-stream for the SBCR and CSTR systems are displayed in Figure 2. The CO conversion for the enhanced SBCR with level control reached a maximum of 78% after 72 hours time-on-stream (TOS). After this catalyst initiation period, the gas conversion started to steadily decline to about 72% after 192 hours TOS.

Slurry back-mixing in the SBCR is significantly reduced by the addition of the down-comer/dip-tube flow path; consequently, the gas and liquid phases likely exhibited more “plug-flow” behavior. Thus, for a given space velocity, the enhanced SBCR should yield a higher conversion than that of a CSTR [5]. Differences in conversion between the enhanced SBCR and CSTR reactor types may also be caused by the dissimilarity of heat and mass transfer phenomena.

SBCR Catalyst Attrition. Heavy wax products must be separated from catalyst particles before being removed from the reactor system. Achieving an efficient wax product separation from the catalyst is one of the most challenging technical problems associated with slurry-phase

F-T. The breakdown of the catalyst particles and the production of heavy wax using high alpha catalysts can further exasperate the filtration problem. Thus, designing a physically robust catalyst without compromising activity is an important factor for a stable and economical F-T process. However, small-scale catalyst attrition tests may not be adequate in simulating the environment within a bubble column reactor. In previous studies [6,7] by Jothimurgean and Zhao an air-jet attrition tester as outlined in the ASTM-D-5757-95 test method was used to compare the relative breakdown resistance of catalysts. This method is useful in comparing the relative strength between catalyst candidates; however, it does not yield information as to the rate of attrition during synthesis. Attrition data in CSTR systems are compromised by the extreme impact and shear forces from the impeller blade on catalyst particles. In contrast, the SBCR unit does not utilize any mechanical pumping devices that could alter the size distribution of the catalyst. Consequently, SBCR particle attrition will depend mainly on chemical changes within particles and perhaps some particle/wall or particle/particle mechanical abrasion.

Figure 3 shows the changing distribution of catalyst concentration with TOS. During the start of activation, only a small fraction of catalyst fines were detected in the reactor effluent stream. However, near the bottom of the reactor the concentration of catalyst particles was greater than 25 wt%. This indicated the liquid recirculation rate was not sufficient to fully entrain the largest (>23 mm) catalyst particles. As the activation process was completed (TOS = 0), the slurry effluent contained about 5 wt% of catalyst fines. Thereafter, the solids concentration of the reactor effluent increased linearly with TOS.

The mean particle size of the reactor bottom and effluent streams are shown in Figure 4. The dotted horizontal line represents the initial mean particle size of the raw catalyst. Physical classification of the catalyst particles was apparent as evidenced by the mean particle size of

slurry in the bottom being greater than that of the raw catalyst. As the synthesis progressed, the mean particle size in the reactor dropped below the baseline (23 μm) after only 40 hours TOS. In summary, the data shown in Figures 3 and 4 indicate that a significant portion of the catalyst exited the reactor system due to particle attrition after 40 hours of TOS. Considering the slurry hold-up outside the reactor was maintained at less than 1 liter, the percentage of catalyst lost after 40 hours TOS was less than 20 wt%. Therefore, this lost catalyst must be considered when calculating the space velocity.

Conclusions

Tight control of catalyst distribution within SBCRs should be maintained in order to quantify activity decline, especially for small pilot plant systems. Transient problems with previous SBCR experiments were caused by a maldistribution of catalyst between the reactor and slurry filtration system. The level indication/control system installed in an enhanced SBCR was robust and effective in maintaining a steady inventory of catalyst slurry in contact with the gas-phase. Measured deactivation rates in the enhanced SBCR system were comparable to that of CSTR experiments under similar conditions.

Attrition tests in the SBCR system indicated that the most of the catalyst breakdown occurred during catalyst activation and the initial synthesis stage; however, further research will be required to investigate the possibility of particle size classification/segregation at the sampling points. After activation, the catalyst particle mean diameter decreased in an exponential decay fashion. Attrition effects must be considered in order to accurately estimate the space velocity in pilot-scale SBCRs.

References

1. R. J. O'Brien, R., L. Xu, D. Milburn, Y. Li, K. Klabunde, and B. Davis, *Top. Catal.* 1995, 2, 1.
2. O'Brien, R., L. Xu, R. L. Spicer, and B. H. Davis, *Energy & Fuels*, 10 (1996) 921.
3. Marretto, C. and R. Krishna, "Modeling of Bubble Column Slurry Reactor for Fischer-Tropsch Synthesis", *Catalysis Today* 52 (1999) 279-289.
4. McCartney, J.T., L. Hofer, B. Seligan, J. Lecky, W. Peebles, and W. Anderson, *J. Phys. Chem.* 1953, 57, 730.
5. Fogler, H., *Elements of Chemical Reaction Engineering*, 1st Edition, pgs. 273-278, Prentice-Hall, Englewood Cliffs, New Jersey 07632, 1986, ISBN 0-13-263476-7.
6. Jothimurugesan, K., J. Goodwin, Jr., S. Gangwal, and J. Spivey, "Development of Fe Fischer-Tropsch Catalysts for Slurry Bubble Column Reactors", *Catalysis Today* 58 (2000) 335-344.
7. Zhao, R., J. Goodwin, Jr., K. Jothimurugesan, S. Gangwal, J. Spivey, "Spray-Dried Iron Fischer-Tropsch Catalysts. 1. Effect of Structure on the Attrition Resistance of the Catalysts in the Calcined State", *Ind. Eng. Chem. Res.* 2001, 1065-1075.

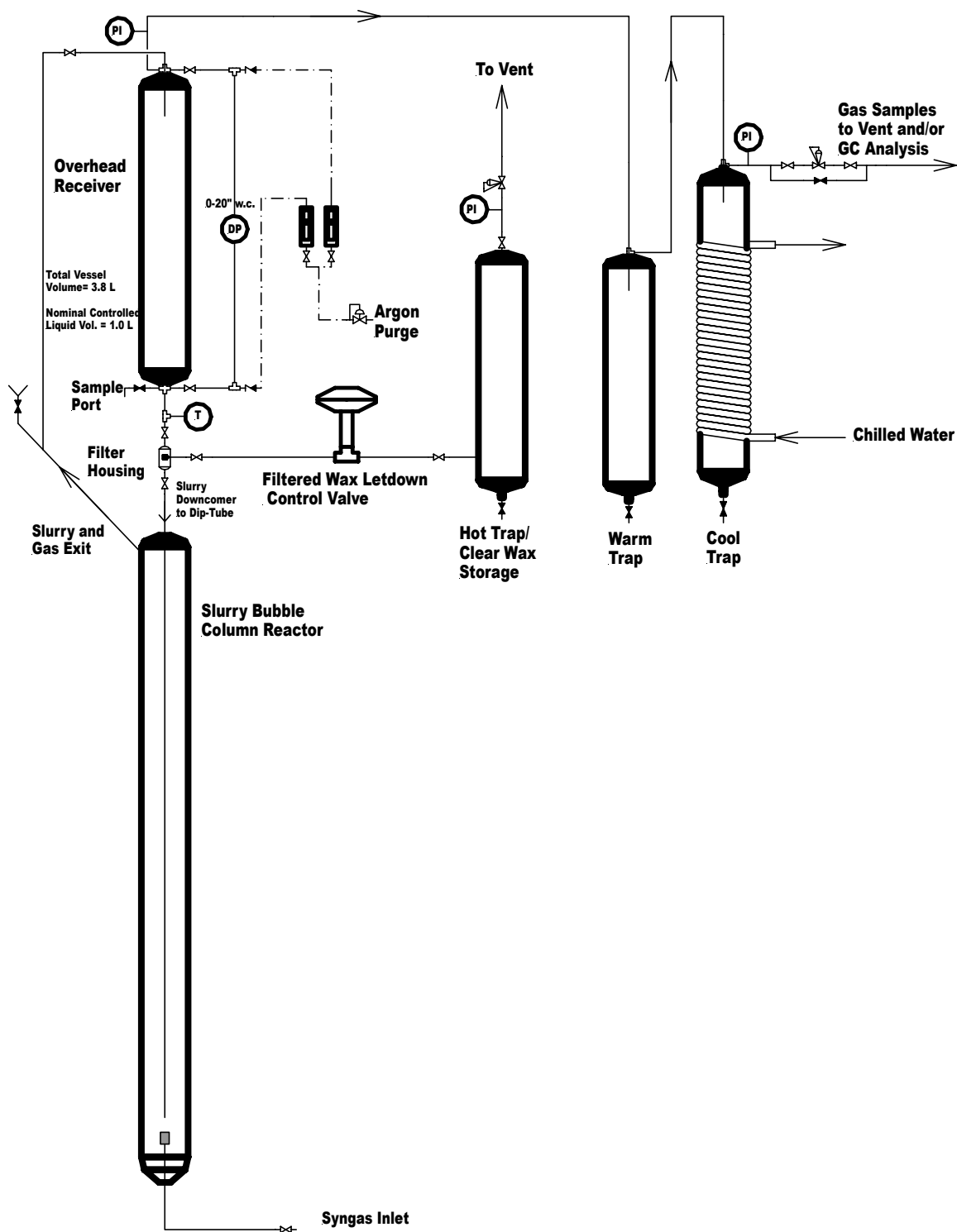


Figure 1. Schematic of SBCR Pilot Plant System

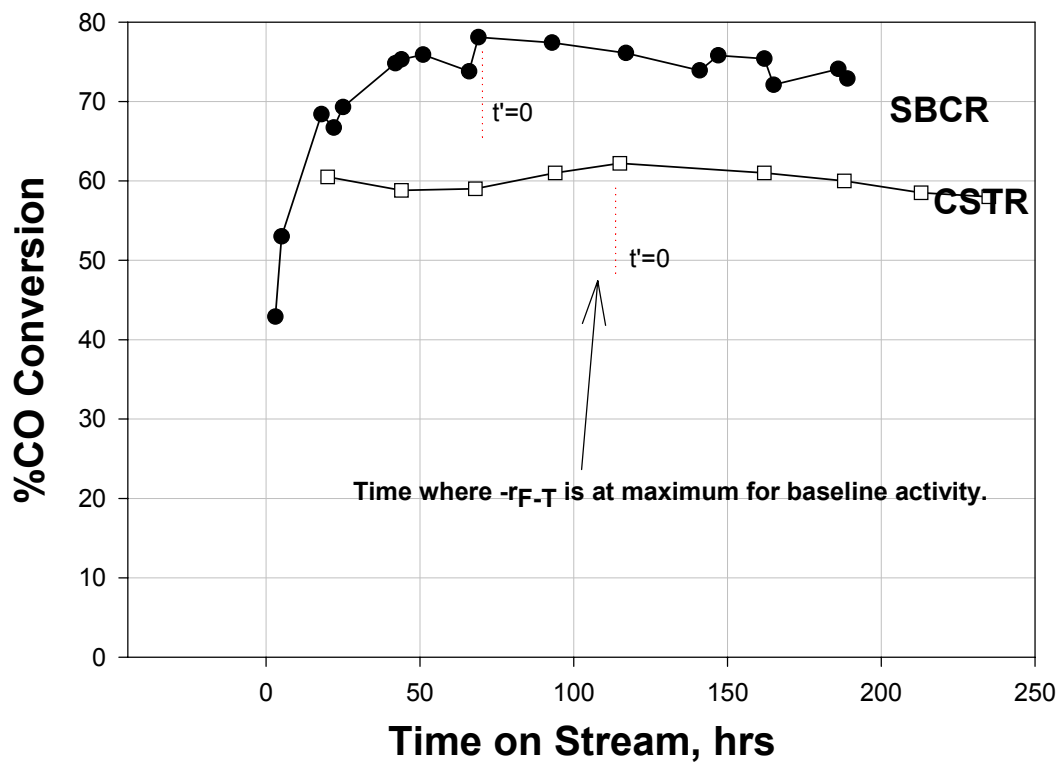


Figure 2. CO conversion comparison between reactor types.

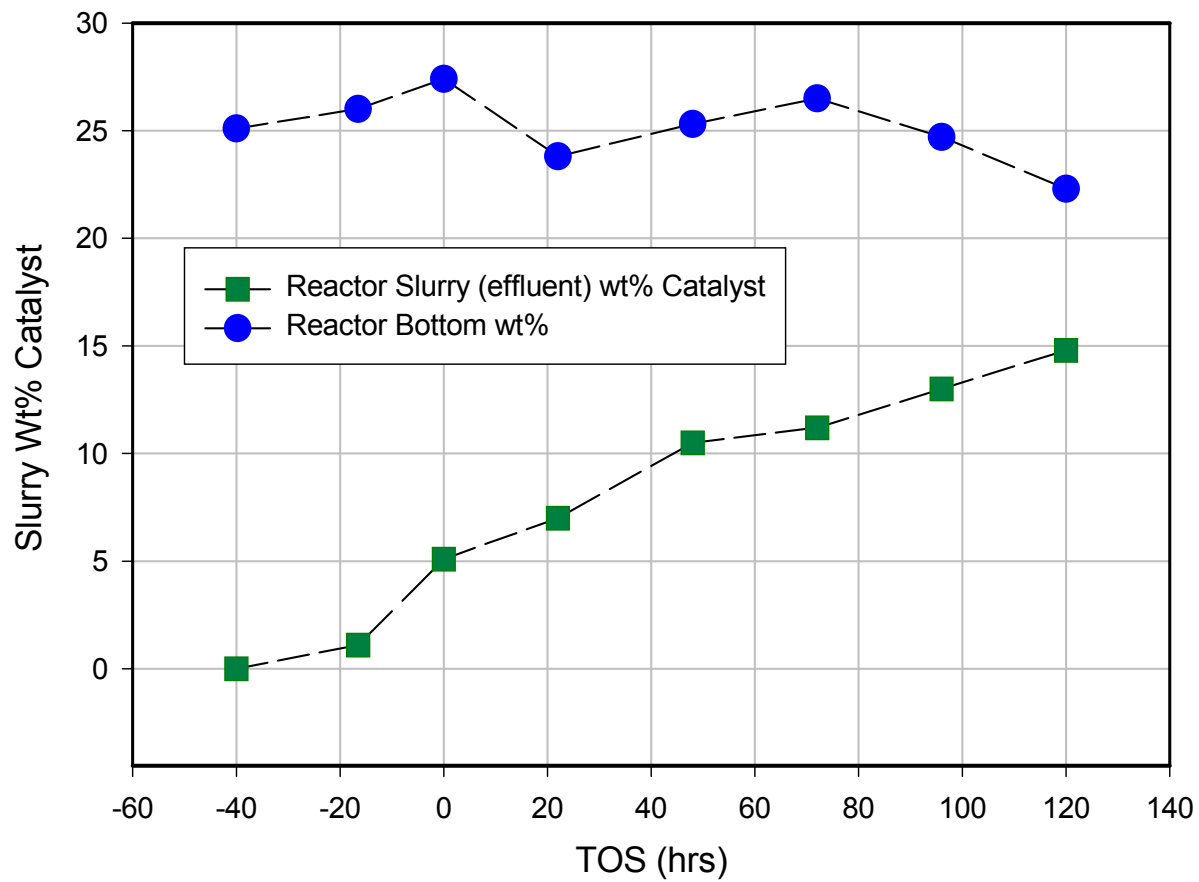


Figure 3. Catalyst solids distribution (reactor and reactor effluent) vs. time-on-stream.

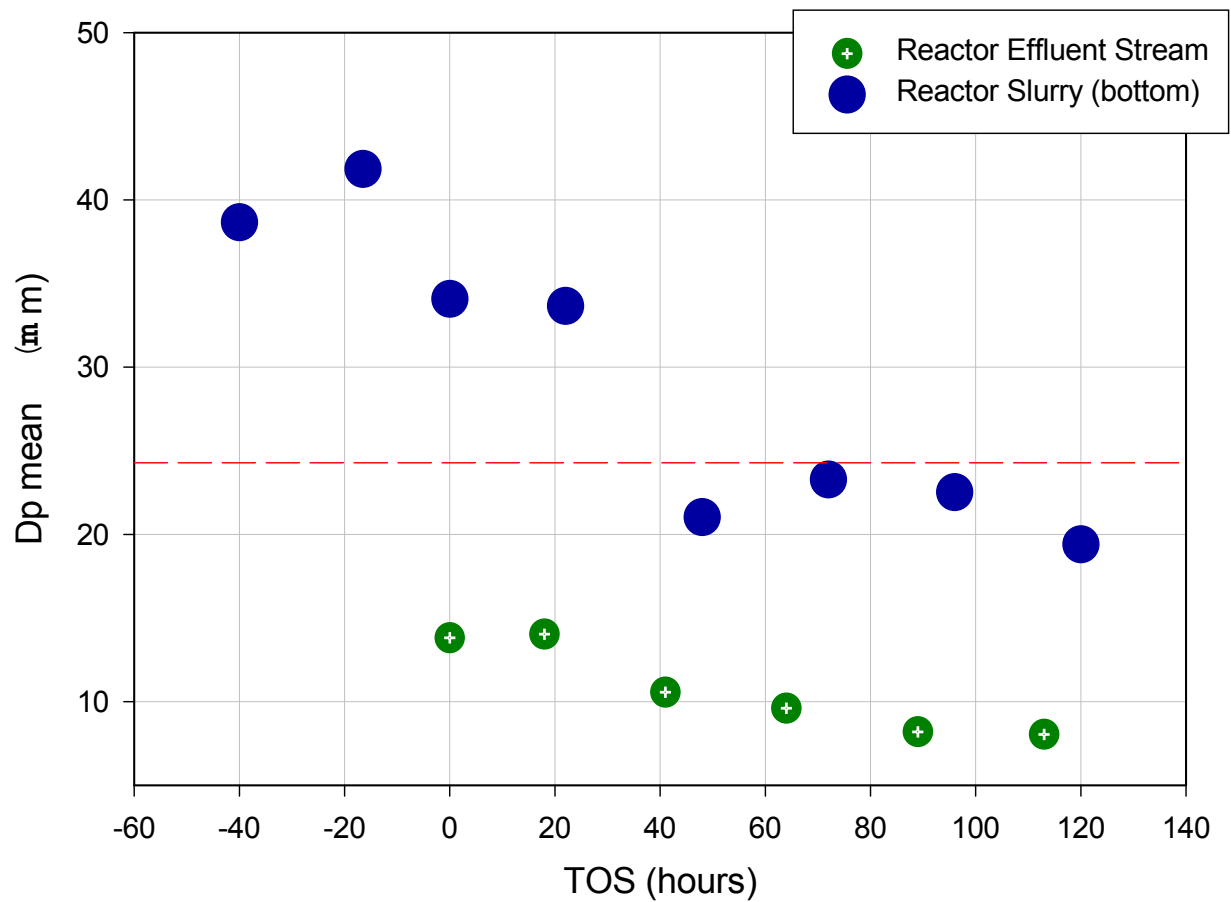


Figure 4. Mean particle size in the catalyst slurry vs. time-on-stream (reactor and reactor effluent).

Task 3. Catalyst Characterization

The objective of this task is to obtain characterization data of the prepared catalysts using routine and selected techniques.

No scheduled or further activity to report.

Task 4. Wax/Catalyst Separation

The objective of this task is to develop techniques for the separation of catalysts from FT reactor slurries.

No scheduled or further activity to report.

Task 5. Oxygenates

The objective of this task is to obtain a better understanding of the factors that affects catalyst selectivity toward oxygenates for iron-based Fischer-Tropsch catalysts.

No scheduled activity to report.

Task 6. Literature Review of Prior Fischer-Tropsch Synthesis with Co Catalysts

The objective of this task is to prepare a critical review of prior work on cobalt Fischer-Tropsch catalysts.

Task completed.

Task 7. Co Catalyst Preparation

The objective of this task is to prepare a limited number of cobalt-based Fischer-Tropsch catalysts that can be used to obtain baseline data on cobalt-based Fischer-Tropsch synthesis.

No scheduled activity to report.

Task 8. Cobalt Catalyst Testing for Activity and Kinetic Rate Correlations

The objective of this task is to conduct initial screening of the cobalt catalysts prepared in Task 7 to select three baseline catalysts that will then be used to generate a data base on the performance of cobalt-based Fischer-Tropsch catalysts in slurry reactors.

A. Fischer-Tropsch Synthesis: Supercritical Conversion Using a Co/Al₂O₃ Catalyst in a Fixed Bed Reactor

Abstract

A cobalt catalyst (25%Co/ γ -Al₂O₃, prepared by slurry phase impregnation) was used in a fixed bed reactor under a pressure/density tuned supercritical fluid mixture of n-pentane/n-hexane. By using an inert gas as a balancing gas to maintain a constant pressure, the density of the supercritical fluid could be tuned near the supercritical point while maintaining constant space velocity within the reactor. The benefits of the mixture allowed for optimization of transport and solubility properties at an appropriate reaction temperature for Fischer Tropsch synthesis with a cobalt catalyst. There was an important increase in conversion due to greater accessibility to active sites after extraction of heavy wax from the catalyst, and additional benefits included decreased methane and carbon dioxide selectivities. Decreased paraffin/(olefin + paraffin) selectivities with increasing carbon number were also observed, in line with extraction of the hydrocarbons from the pore. Removal of the wax products resulted in lower residence times in the catalyst pores and, therefore, decreased probability for readsorption and reaction to the hydrogenated product. Even so, there was not an increase in the alpha value over that obtained with just the inert gas.

1. INTRODUCTION

In the near future, increasing dependence on stranded natural gas reserves for fuel production is expected. This combined with increasing political pressure on oil companies to limit flaring of gas has renewed focus on Gas-to-Liquids (GTL) technology. Most GTL plants considered for commercialization consist of three process steps: (1) synthesis gas production from natural gas; (2) Fischer-Tropsch synthesis (FTS) to convert syngas to a crude hydrocarbon mixture (syncrude); and (3) hydroprocessing of syncrude to transportation fuels. Due to the perception of high activity and stability, the catalyst of choice for FTS is typically a supported cobalt catalyst.

There are positive features as well as drawbacks to conducting Fischer-Tropsch by the traditional gas phase route or even by the more advanced liquid phase methods. For example, gas phase FTS, which is typically carried out in a fixed or fluid bed reactor, produces higher initial product yields, due to the superior catalyst concentration per reactor volume. However, these higher initial rates, coupled with the potential for poor heat removal capacities of fixed-bed gas phase processing, typically lead to localized overheating of the catalyst, due to the exothermicity of the reaction, resulting in sintering of cobalt clusters, as well as the deposition of heavy waxes within catalyst pores, both contributing adversely to catalyst deactivation.

Better heat control throughout the reactor can be gained by conducting FTS in the liquid phase, due to the better heat removal capacities of the liquid. Liquid phase FTS is typically run in the laboratory as a continuously stirred tank reactor (CSTR) or commercially in the more slurry bubble column reactor (SBCR). In addition, deactivation rates are lower, because the liquid media facilitates dissolving wax products, both internal and external to the catalyst pores. However, the liquid itself provides a resistance to the diffusional transport of gas phase reactants to active sites, resulting in a possible decrease of the reaction rate in comparison to gas phase

FTS. Also, separation of the attrited catalyst fines from the waxy product remains problematic for liquid phase FTS in comparison to the typical fixed bed gas phase reactor, whereby the wax products typically trickle down the catalyst bed.

By conducting FT in supercritical media [1], where the supercritical fluid is usually a relatively low molecular weight solvent, one may take advantage of both the gas-like transport properties as well as the liquid-like heat capacity and solubility characteristics of the supercritical fluid, and utilize the fixed bed reactor. Implementing a fixed bed supercritical reactor process may achieve two important goals of improving the economics of GTL operations: (1) catalyst lifetimes can be extended by suppressing deactivation by pore plugging via heavy molecular weight wax products and (2) the requirement of filtration to effect the removal of the wax product, as is needed for CSTR and SBCR operations, is avoided.

A 25%Co/ γ -Al₂O₃ catalyst, prepared using a slurry phase impregnation method, was found to exhibit high activity and stability in a CSTR (H₂/CO = 2, T = 220°C, P= 1.9 MPa). Considerable effort was made to stabilize the catalyst against deactivation by reoxidation and other instabilities, which occur when the cluster size of cobalt is below about 10 nm [2,3].

Choice of supercritical fluid, in our case a mixture, was based on, with some modification, the following criteria set forth by Fujimoto et al. [4]:

1. The critical temperature and pressure should be slightly lower than the typical reaction temperature and pressure. In this case, reaction temperature was similar to normal FTS, but the reactor total pressure (8.24 MPa) was considerably higher than used for either a gas-phase or liquid phase FTS reactor (approximately 2.00 MPa). Although much less sensitive to total pressure than temperature, FTS is reported to shift to produce heavier

products with an increase in the total pressure of syngas [5]. This pressure dependence is more pronounced for cobalt than for an iron catalyst [Sasol].

2. The solvent should be one which does not poison the catalyst and should be stable under the reaction conditions. The low molecular weight paraffins chosen for this study are unreactive and stable. Also, the paraffins are not coke precursors under the mild temperatures of FTS.
3. The solvent should have a high affinity for aliphatic hydrocarbons to extract the wax from the catalyst surface and reactor.

Because the upper optimum temperature for FTS for cobalt catalysts is approximately 220°C, the critical temperature of the solvent was selected to be below this temperature. In a previous study [6] by our group, and reproduced here in Figures 1 and 2, it was determined using the Hysys 2.1 process simulator that a 55% hexane/45% pentane mixture should give favorable liquid-like densities, while still maintaining gas-like transport properties at a pressure of approximately 8.24 MPa. Using these conditions with the 25%Co/Al₂O₃ catalyst, supercritical studies were conducted by varying the partial pressure of the supercritical fluid, maintaining constant space velocity by using argon as a balancing gas, to determine if the increased solubility of the wax products in the supercritical fluid improved the activity and deactivation profile during reaction testing.

2. EXPERIMENTAL

2.1 Catalyst Preparation

Condea Vista Catalox (high purity γ -alumina, 100-200 mesh, 175 m²/g) was used as the support material for the cobalt FTS catalyst. The catalyst was prepared by a slurry impregnation method, and cobalt nitrate was used as the precursor. In this method, which follows a Sasol

patent [7], the ratio of the volume of solution used to the weight of alumina was 1:1, such that approximately 2.5 times the pore volume of solution was used to prepare the loading solution. Two impregnation steps were used, each to load 12.5% of Co by weight. Between each step the catalyst was dried under vacuum in a rotary evaporator at 333 K and the temperature was slowly increased to 373 K. After the second impregnation/drying step, the catalyst was calcined under air flow at 673K.

2.2 *BET Measurements*

The surface areas of the support and catalyst were measured by BET using a Micromeritics Tri-Star system. Prior to the measurement, the sample was slowly ramped to 433K and evacuated for 4hrs to approximately 6.7 Pa. Results of physisorption measurements are shown in Table 1.

2.3 *Hydrogen Chemisorption with Pulse Reoxidation*

Hydrogen chemisorption measurements were performed using a Zeton Altamira AMI-200 unit, which incorporates a thermal conductivity detector (TCD). The sample weight was 0.220 g. The catalyst was activated at 623K for 10hrs using a flow of pure hydrogen at atmospheric pressure and then cooled under flowing hydrogen to 373K. The sample was held at 373 K under flowing Ar to prevent physisorption of weakly bound species prior to increasing the temperature slowly to 623K. At that temperature, the catalyst was held under flowing Ar to desorb the remaining chemisorbed hydrogen so that the TCD signal returned to the baseline. The TPD spectrum was integrated and the number of moles of desorbed hydrogen determined by comparing to the areas of calibrated hydrogen pulses. Prior to experiments, the sample loop was calibrated with pulses of N₂ in helium flow and compared against a calibration line produced from gas tight syringe injections of N₂ under helium flow.

After TPD of H₂, the sample was reoxidized at 623K by injecting pulses of pure O₂ in helium referenced to helium gas. After oxidation of the cobalt metal clusters, the number of

moles of O₂ consumed was determined, and the percent reducibility calculated assuming that the Co⁰ reoxidized to Co₃O₄.

2.4 Temperature Programmed Reduction

The temperature programmed reduction (TPR) profile of the fresh catalyst was obtained using a Zeton Altamira AMI-200 unit (Figure 3). The calcined fresh sample was first heated and purged at 473K in flowing Ar to remove traces of water. TPR was performed using 30 cc/min 10% H₂/Ar mixture referenced to Ar. The ramp was 5K/min from 303K to 623K, and the sample was held at 623K for 30 min.

2.5 X-ray Diffraction

The powder diffractogram of the calcined catalyst was recorded using a Philips X'Pert diffractometer. First, short-time scans were taken over the range from 2θ of 20° to 70° to verify the formation of Co₃O₄ after calcination. Then, a long-time scan was made over the intense peak at 36.8° corresponding to (311) so that estimates of Co₃O₄ cluster size could be assessed from Scherrer line broadening analysis. The scanning step was 0.01, the scan speed was 0.0025 sec⁻¹, and the scan time was 4 sec.

2.6 Reaction Testing

The plug flow reactor configuration illustrated in Figure 4 was used and operated at a total pressure of 8.24 MPa. The amount of catalyst was 3 g, diluted in 15 g of glass beads (80-100 mesh). Temperature control was achieved using a three heating-zone furnace. Reactant feed gases (H₂ and CO; H₂:CO of 2:1), as well as argon balancing gas and nitrogen calibration gas, were introduced into the reactor by Brooks 5850 mass flow controllers, which were calibrated over a wide range of pressure for the gases used. The solvent, a mixture of 55% hexane and 45% pentane (by volume), was introduced to the reactor using an Altex Model 110A liquid feed pump.

The configuration, with dual hot and cold traps, allowed for switching of the product stream in order to maintain the reactor under normal operation and system total pressure during sample collection. The traps were maintained at 423K and 273K, respectively. In addition, a dry ice/acetone trap was brought online as necessary. Since sampling of the oil, liquid, and supercritical fluid caused a substantial drop in the pressure of the traps, prior to restoring the traps online, they were repressurized to system pressure using argon as the inert gas. This complicated the gas analysis, since the gas stream from the traps was diluted by the argon used to bring the traps back to operating pressure. To solve this problem and assess CO conversion, inert N₂ gas was used for calibration, as follows:

For the reactor:

$$X_{CO} = (N_{CO, in} - N_{CO, out}) / (N_{CO, in})$$

$$X_{CO} = [(V_{in})(y_{CO, in}) - (V_{out})(y_{CO, out})] / [(V_{in})(y_{CO, in})]$$

In the calculation, N_{CO, out} refers to the moles of CO exiting the reactor, not the traps, which are diluted. Nitrogen is unreactive and, therefore, the molar flow of nitrogen will be the same entering and exiting the reactor. So, to correct for the argon dilution of the traps, nitrogen is used to calibrate as follows.

For the traps:

$$\text{calibration factor} = C_F = \text{molar flow}_{N_2, in} / \text{molar flow}_{N_2, out}$$

$$C_F = [(V_{in})(y_{N_2, in})] / [(V_{out})(y_{N_2, out})]$$

$$X_{CO} = [(V_{in})(y_{CO, in}) - (V_{out})(y_{CO, out})(C_F)] / [(V_{in})(y_{CO, in})]$$

Note that the molar flow of nitrogen entering the trap is the same as the molar flow of nitrogen exiting the reactor, which is the same as the molar flow of nitrogen entering the reactor. Therefore, all quantities are easily measured. Trap outlet gas flows were measured using a wet

test meter. This procedure was implemented to address problems encountered in our earlier work [6].

As another means to calculate the conversion, the CO:N₂ ratio was analyzed both before entering and after reaction, as follows.

$$X_{\text{CO}} = 1 - (\text{N}_2/\text{CO})_{\text{in}}/(\text{N}_2/\text{CO})_{\text{out}}$$

Organic phase condensed liquid products of Fischer-Tropsch synthesis were analyzed by gas chromatography. The analyses of C₅ - C₃₀ hydrocarbons were performed on a Hewlett Packard (HP 5890) Gas Chromatograph equipped with a capillary column DB-5 (length: 60m, i.d.: 0.32 mm and film thickness: 0.25 micrometer), He as a carrier gas and FID, and operated with temperature programming from 308-598K at 4K/min. The analyses of reactor wax were performed on a Hewlett Packard (HP 5890) Gas Chromatograph equipped with a capillary column (length: 25m, i.d.: 0.53 mm and film thickness: 0.15 micrometer), He as a carrier gas and FID with temperature programming from 323-663K at 10K/min. The product data were handled using Hewlett-Packard Chemstation data analysis software.

3. RESULTS AND DISCUSSION

3.1 *Characterization*

To obtain an estimate of the Co⁰ cluster size by adsorption methods, it is necessary to first determine the fraction of the cobalt that is reduced during activation of the catalyst. It is not unusual to use the weight of the catalyst and the percentage of metal to determine the number of metal atoms in the sample, and place this in the denominator for the dispersion calculation. However, the TPR profile in Figure 3 indicates that not all of the cobalt is reduced during activation at 623K; thus, a pulse reoxidation method was used to quantify the percentage reduction, a method that has been used extensively in characterizing cobalt catalysts for Fischer-

Tropsch synthesis [8]. To estimate the cluster size, the following equations are used, and the results for hydrogen TPD/pulse reoxidation are shown in Table 2.

$$\%D = (\#\text{Co}^0 \text{ atoms on surface} \times 100\%) / (\text{total } \#\text{Co}^0 \text{ atoms})$$

$$\%D = (\#\text{Co}^0 \text{ atoms on surface} \times 100\%) / [(\text{total } \#\text{Co atoms in sample})(\text{fraction reduced})]$$

After calcination of the catalyst, the phase of cobalt detected by XRD was the spinel structure of Co_3O_4 . To provide another estimate of the cobalt cluster size, the calcined catalyst was scanned by X-ray diffraction. Scherrer line broadening analysis by determination of the full width at half the maximum (FWHM) of the peak at 36.8° was used to estimate the average size of the Co_3O_4 clusters. After reduction, the metal cluster size should be approximately 75% of this size.

Therefore, as displayed in Table 2, there is very good agreement between the results based on calculations using chemisorption with reoxidation data and the results based on calculations based on XRD data.

3.2 *Reaction Testing*

There has been great interest in utilizing the unique physical and transport properties of fluids near their critical pressures and temperatures, as they can be made either more gas-like or liquid-like by pressure tuning. With pressure tuning of the supercritical fluid, solubilities can be enhanced to facilitate the dissolution and removal of wax products from the catalyst, while maintaining gas-like diffusional properties of the reactants CO and H_2 through the elimination of interphase transport limitations on the reaction rate [9]. Figure 2 reveals that the density change from gas-like to liquid-like occurs between 1 and 6 MPa. Most previous studies of Fischer-Tropsch synthesis in the literature have focused on using pure solvents as supercritical fluids [10-12]; therefore, the solvents in these studies were not at the optimum conditions for FTS. For example, n-hexane has been used [10,11], with critical properties $T_c = 506.7 \text{ K}$ and $P_c = 2.97 \text{ MPa}$, but the temperature of the reactor must be operated at approximately 513 K, a temperature

which is too high for cobalt-based FTS catalysts and favors production of light products. Also, n-pentane, with critical properties $T_c = 196.6$ and $P_c = 3.33$ MPa, was also used in previous work, but the density is not high enough to attain optimum solubility properties at the FTS conditions. Propane was also used [12], with the same problem.

Among, if not the first, group to study the pressure tuning affect of the solvent pressure on the transport and solubility properties was Subramaniam [11]. In that work, the pressure of the reactor was changed, while the CO/H₂ ratio of the gas feed and supercritical liquid feeds were kept constant. The partial pressures and the residence times were altered with each change of condition and make it difficult to draw solid conclusions.

As an extension to this previous work, efforts were made to overcome the above problems. In this work, a constant overall reactor pressure and constant partial pressures of the feed CO and H₂ gases were maintained. [We refer to nonsupercritical conditions although the inert gases are present at supercritical but very low density conditions.] Only the partial pressure of the supercritical fluid mixture is changed to tune the transport and solubility properties, while a balancing inert gas (argon) is fed to maintain constant space velocity. Nitrogen is also fed, but it is used as a calibration gas, so that CO conversion can be accurately assessed.

The data in Figure 5 show that when no or inadequate partial pressures of supercritical fluid are present, the catalyst undergoes deactivation, probably by heavy wax buildup. However, when the partial pressure of the supercritical fluid was 5.45 MPa, an increase in CO conversion was observed due to the increased solubility of wax products in the supercritical media. It was further noted that the amount of wax products sampled from the collection traps increased dramatically, and then leveled off, consistent with wax extraction, as shown in Figure 6.

In practice, the chain growth probability α is used to define distribution of product selectivity, based on Anderson-Schulz-Flory (ASF) polymerization kinetics, as follows:

$$\alpha = R_p / (R_p + R_t)$$

where R_p and R_t are the rates of chain propagation and termination. Therefore, except for deviations from this ideal model, with methane showing much higher termination probabilities yielding higher than predicted values, and C_2 products giving lower than predicted values [13], these kinetics define the distribution of products based on carbon number, n . In contrast with Fe-based FTS catalysts, the distribution of components for cobalt catalysts strongly favors paraffins, although measurable quantities of olefins and traces of oxygenated products are also present, primarily in lower carbon number components. In this study, the products were lumped into the parameter m_n , representing the sum of the components for each carbon number, where:

$$m_n = (1 - \alpha)\alpha^{n-1}$$

Therefore, the slope of the natural log of the mole fraction versus the carbon number yields α as follows:

$$\alpha = \exp[\Delta \ln m_n / \Delta n]$$

Table 3 and Figure 7 show that the resulting α value was very close to the value obtained during CSTR testing, and remained constant during the course of reaction testing with or without supercritical fluid, with values ranging between 0.87 and 0.90%.

Product selectivities were determined in two ways, as commonly reported in the literature. Methane selectivity was defined on a carbon molar basis, not on a product molar basis, and CO_2 from the water-gas-shift reaction was not included. C_5+ selectivity was defined in a similar manner. In contrast, the CO_2 selectivity was based on the rate of water-gas-shift

divided by the rate of water-gas-shift plus the FTS rate, again on a carbon molar basis, as follows:

$$S_{\text{CH}_4} = r_{\text{CH}_4}/r_{\text{FTS}} = r_{\text{CH}_4}/(r_{\text{CO}} - r_{\text{CO}_2})$$

$$S_{\text{C}_{5+}} = r_{\text{C}_{5+}}/r_{\text{FTS}} = r_{\text{C}_{5+}}/(r_{\text{CO}} - r_{\text{CO}_2})$$

$$S_{\text{CO}_2} = r_{\text{CO}_2}/(r_{\text{CO}_2} + r_{\text{FTS}}) = r_{\text{CO}_2}/r_{\text{CO}}$$

The C₂+ total olefin selectivity was defined on a carbon molar basis. First, the olefin selectivity for each carbon number was calculated, as follows:

$$S_{\text{O},n} = \text{O}/(\text{O}+\text{P})_n$$

Then, the C₂+ total olefin selectivity “C₂⁼⁺” was determined by integrating over the distribution up to C₂₀.

$$C_{2}^{=+} = \frac{\sum S_{\text{O},n} \alpha^n n}{\sum \alpha^n n}$$

Initially, there are not important differences between the catalyst run with or without supercritical fluid because early in the run, the catalyst is relatively free of wax products as it is in the initial stage of deactivation. However, as shown in Table 3 and Figure 8, after the deactivation period and especially under the condition of no supercritical hydrocarbon addition during days 15 - 20, the CO₂ selectivity is approximately 10% and the methane selectivity is greater than 15%. This is the most important time to observe the differences between supercritical and non-supercritical conditions, at the point where the catalyst has deactivated by wax buildup. Clearly, after switching to the supercritical fluid partial pressure of 5.45 MPa, important benefits in product selectivity occurred, with notable decreases in the selectivities of both CO₂ and methane.

CO₂ is produced by the water-gas-shift reaction: H₂O + CO ⇌ CO₂ + H₂. Yokota et al. [14] attributed the decrease in CO₂ production over an iron-based catalyst to the improved

extraction and transport of water by the supercritical fluid. This implies that the residence time of the H₂O relative to the reactants H₂ and CO in the reactor was shortened yielding a lower production rate of CO₂. Our results are consistent with this explanation.

The methane selectivity is highly sensitive to changes in the process parameters. Increasing temperature, decreasing the pressure, increasing the H₂:CO, and changing the conversion all may result in an increase in methane selectivity for cobalt catalysts [13, 15, 16]. In this work, we attempted to maintain constant all parameters in our control in order to make comparisons under supercritical and nonsupercritical conditions. After deactivation of the catalyst by wax buildup, during days 15-20 under nonsupercritical conditions, the methane selectivity is high (greater than 15%). However, when the 5.45 MPa of the SCF is added, the methane selectivity decreases while the conversion increases. Therefore, one could assume that the increased availability of active sites after extraction of long chain wax from the pores resulting in increased conversion could decrease the methane selectivity. Another explanation is that the observed decreased methane selectivity is the result of better heat distribution in the reactor. That is, under supercritical conditions, localized hotspots in the reactor are avoided [17] due to the better heat capacities of the SCF, resulting in lower methane selectivities. In that case, one would also expect an increase of the chain growth parameter α . However, in Table 3, very little, if any, change in α is observed with or without addition of supercritical fluid. Another explanation is that mass transfer limitations are decreased with addition of the SCF due to the improved extraction of the FTS products from the catalyst. The slow transport of heavy wax products from the catalyst contribute to the deactivation of the catalyst and may increase the mass-transfer limitations when no SCF is present. Therefore, this could also explain the increase of methane selectivity with time onstream, since it is well known that mass transport limitations

can result in an increase of the thermodynamically favored product methane [18]. When a high enough density of SCF is achieved (5.45 MPa) and solubilization of the wax occurs, resulting in extraction, it is possible that the mass transfer barrier is decreased, resulting in the decreased methane selectivity.

That wax extraction occurred is also evident when one considers the selectivity of olefins to paraffins with increasing carbon number. These are reported in Table 4 for both conditions - with or without SCF, and with changes in the SCF partial pressure. There is currently a debate in the literature as to the cause of the decrease in olefin content with higher carbon number for FTS. One is the higher solubility of higher carbon number product α -olefins in the liquid phase, resulting in increased residence times which lead to their increased reactivity. Henry's law constants, which indicate the fugacity (in many cases, partial pressure) of a component in the gas phase divided by the concentration of the solute gas in the liquid phase, have been observed for paraffins to decrease exponentially with carbon number, indicating higher solubility with carbon number [13]. Therefore, several authors [e.g., 13] have advanced the view that the greater solubility of larger hydrocarbons result in increased residence times and therefore, higher rates of readsorption.

However, a different explanation was offered [19-23]. The decrease in olefin content with carbon number in this view is due to the decrease in the diffusivities of longer chain hydrocarbons, which would lengthen their time in the catalyst pores. This has been coined "diffusion enhanced α -olefin readsorption."

The results presented here show that with the addition of SCF, the paraffin content is much lower with increasing carbon number than without SCF. Therefore, the diffusivities of hydrocarbons may be much higher in the presence of the supercritical fluid. This could result in

lower residence times in the pores, and therefore, decreased probability for readsorption. Certainly, this is a possible explanation for the results. However, a more likely explanation is based on a VLE study [24]. Based on a reaction scheme which took into account reversibility of both olefin hydrogenation and adsorption and derived from material balances, it was demonstrated that the residence time of each carbon number was inversely related to the saturated vapor pressure. Moreover, the olefin to paraffin ratio was inversely related to the residence time. Therefore, the results here may be explained in terms of this model. When no SCF is present, $O/(O+P)$ decreases with carbon number due to the higher residence times of the higher carbon number intermediates resulting from their lower saturation vapor pressures. With addition of SCF, extraction results in removal of the liquid layer, which results in a decrease of the residence time of intermediates and an increase in $O/(O+P)$ as a function of carbon number relative to the nonsupercritical condition, as shown in Figures 8 and 9, and Table 4.

The research may also lead to other developments. For example, reaction intermediates could potentially be added to the supercritical fluid in order to achieve incorporation into the wax products. For example, Fujimoto's group [25] has extended the idea to explore the addition of middle α -olefins to promote wax selectivities. Also, our group has added ^{14}C labeled α -olefin compounds to the supercritical fluid in order to test the merits of α -olefin reincorporation [26].

4. CONCLUSIONS

The anticipated benefits of running FTS in a supercritical fixed bed reactor are clear. In comparison with gas phase fixed bed processes, by using well pressure tuned supercritical media, in this case a C_5/C_6 mixture, the condensation of high molecular weight hydrocarbons leading to catalyst deactivation was avoided. In contrast to conventional slurry phase processes, which suffer from catalyst attrition, whereby the catalyst fines eventually breakdown to the point

at which they can channel through the filter, running FTS under the supercritical media avoided this problem altogether. With the increase in conversion due to greater accessibility to active sites after wax extraction, additional benefits included decreased methane and carbon dioxide selectivities. The decreased paraffin/(olefin + paraffin) selectivities with increasing carbon number was in line with extraction of the hydrocarbon from the pore. Two possibilities are considered. Faster diffusion rates of wax products may result in lower residence times in the pores, and therefore, decreased probability for readsorption and reaction to the hydrogenated product. A more probable explanation is that the residence times of intermediate olefins, which are inversely related to their saturation vapor pressures, are decreased due to removal of the liquid phase during extraction.

REFERENCES

1. Baiker, A., Chem. Rev. 99 (1999) 453.
2. Schanke, D., Hilmen, A.M., Bergene, E., Kinnari, K., Rytter, E., Adnanes, E., and Holmen, A., Catal. Lett. 34 (1995) 269.
3. Hilmen, A.M., Schanke, D., Hanssen, K.F., and Holmen, A., Appl. Catal A: General 186 (1999) 169.
4. Fan, L., Fujimoto, K., Appl. Catal. A: General 186 (1999) 343.
5. Dry, M.E., Catalysis-Science and Technology (J.R. Anderson and M. Boudart, eds.), Springer-Verlag, New York, 1981, Vol. 1, pp. 160-255.
6. Zhang, Y., Sparks, D.E., Spicer, R.L., and Davis, B.H., Symposium on Advances in Fischer-Tropsch Chemistry, Div. of Petroleum Chemistry, 219th National ACS Meeting, San Francisco, CA (March, 2000).
7. Espinoza, R.L., Visagie, J.L., van Berge, P.J., Bolder, F.H., U.S. Patent 5,733,839 (1998).
8. Vada, S., Hoff, A., Adnanes, E., Schanke, D., and Holmen, A., Topics in Catal. 2 (1995) 155.
9. Savage, P.E., Gopalan, S., Mizan, T.I., Martino, C.J., and Brock, E.E., AIChE Journal 41, No. 7 (1995) 1723.
10. Fan, L. and Fujimoto, K., Appl. Catal. A: General 186 (1999) 343.
11. Subramaniam, B., Symp. on Advances in FTS Chemistry, 219th National Meeting, ACS, San Francisco, (2000) 194.
12. Lang, X., Akgerman, A., and Bukur, D., Ind. Eng. Chem. Res., Vol. 34, No. 1 (1995) 72.
13. Van der Laan, G.P. and Beenackers, A.A.C.M., Catal. Rev.-Sci. Eng., Vol. 41 No. 3&4 (1999) 255.

14. Yokota, K., Hanakata, Y., and Fujimoto, K., Natural Gas Conversion, (A. Homen et al. eds.) (1991) 289.
15. Iglesia, E., Reyes, S.C., and Madon, R.J., J. Catal. 129 (1991) 238.
16. Bukur, D.B., Patel, S.A., and Lang, X., Appl. Catal. A 61 (1990) 329.
17. Yokota, K., Hanakata, Y., and Fujimoto, K., Fuel 68 (1989) 255.
18. Dry, M.E., J. Mol. Catal., 17 (1982) 133.
19. Iglesia, E., Reyes, S.C., and Soled, S.L., "Computer-Aided Design of Catalysts and Reactors", (E.R. Becker and C.J. Pereira, Eds.), Marcel Dekker, Inc., 1992.
20. Iglesia, E., Reyes, S.C., Madon, R.J., and Soled, S.L., Adv. Catal. 39 (1993) 221.
21. Madon, R., Iglesia, E., Reyes, S., Selectivity in Catalysis (1993) 181.
22. Iglesia, E., Stud. Surf. Sci. Catal., 107 (1997) 153.
23. Iglesia, E., Appl. Catal. A 161 (1997) 59.
24. Zhan, X. and Davis, B. H., AIChE Meeting, April 23, 2001.
25. Fan, L., Yoshii, K., Yan, S., Zhou, J., Fujimoto, K., Catal. Today 36 (1997) 295.
26. CAER, unpublished results.

Table 1			
Results of BET Surface Area Measurements			
Catalyst Description	Calcination T (K)	Measured BET SA (m ₂ /g)	Measured Ave. Pore Rad (nm)
Condea Vista γ -Al ₂ O ₃ Catalox SBa-150	623K	149	5.4
25%Co/ γ -al ₂ O ₃ Catalox Sba-150 Slurry	623K	89	4.8

Table 2

Results of H₂ Chemisorption by TPD of H₂ and Pulse Reoxidation for Co/Al₂O₃ Catalysts Compared with Results from XRD by Scherrer Line Broadening Analysis

H ₂ TPD/Pulse Reoxidation										
Catalyst Description	BET SA m ₂ /g	Red T (K)	μmol H ₂ Desorbed per g	Uncorr % Disp	Uncorr Diam (nm)	μmol O ₂ Uptake per g	% Red	Corr % Disp	Corr Co ⁰ Diam (nm)	Co ₃ O ₄ Diam (nm) XRD
25%Co/Al ₂ O ₃	89	623	77.7	3.7	28.2	1174	42	8.7	11.8	13.7

			Average Selectivities			
TOS (days)	Condition	Final CO Conv	CO ₂	CH ₄	C ₅ +	Final α
0 - 3	No SCF	45.3%	2.1%	8.3%	89.7%	0.88%
3 - 5	2.34 MPa SCF	41.9%	4.1%	9.7%	89.3%	0.90%
5 - 7	3.90 MPa SCF	37.9%	5.5%	11.3%	87.4%	0.90%
7 - 9	5.45 MPa SCF	41.7%	4.7%	10.7%	88.4%	0.87%
9 - 11	3.90 MPa SCF	35.9%	5.7%	12.1%	87.1%	0.89%
11 - 12	5.45 MPa SCF	41.8%	5.8%	12.1%	86.8%	0.90%
12 - 15	2.34 MPa SCF	35.9%	7.2%	13.7%	85.0%	0.88%
15 - 20	No SCF	18.9%	10.3%	16.2%	78.9%	0.88%
20 - 29	5.45 MPa SCF	41.2%	4.3%	10.4%	89.0%	0.87%
42 - 26	No SCF	21.3%	4.8%	18.3%	76.0%	---
46 - 53	5.45 MPa SCF	27.9%	2.2%	11.9%	87.2%	—

Table 4									
Olefin Selectivities as a Function of Supercritical Fluid Partial Pressure									
	O/O + P								
P _{SCF} (MPa)	No SCF	2.34	3.90	5.45	3.90	5.45	2.34	No SCF	5.45
TOS (days)	0-3	3-5	5-7	7-9	9-11	11-12	12-15	15-20	20-29
Carbon No.									
2	0.20	0.20	0.16	0.14	0.18	0.13	0.20	0.20	0.11
3	0.70	0.72	0.73	0.71	0.71	0.70	0.73	0.70	0.71
4	---	0.65	0.64	0.67	0.60	0.69	0.61	0.60	0.61
5	---	---	---	---	---	---	---	---	---
6	0.54	---	---	---	---	---	---	---	---
7	0.51	0.49	0.49	0.44	0.44	0.41	0.46	0.55	0.45
8	0.46	0.55	0.59	0.58	0.58	0.58	0.55	0.53	0.58
9	0.40	0.56	0.63	0.62	0.61	0.62	0.61	0.49	0.60
10	0.40	0.47	0.55	0.55	0.60	0.56	0.50	0.44	0.55
11	0.34	0.42	0.50	0.54	0.48	0.53	0.41	0.38	0.54
12	0.29	0.36	0.46	0.52	0.44	0.51	0.36	0.32	0.52
13	0.24	0.30	0.43	0.50	0.40	0.53	0.31	0.25	0.51
14	0.20	0.25	0.38	0.48	0.35	0.56	0.26	0.20	0.48
15	0.17	0.21	0.34	0.45	0.30	0.59	0.21	0.16	0.46
16	0.14	0.16	0.28	0.43	0.26	0.41	0.17	0.13	0.43
17	0.12	0.15	0.25	0.41	0.21	0.39	0.14	0.12	0.42
18	0.10	0.08	0.23	0.37	0.18	0.36	0.13	0.10	0.39
19	0.09	0.07	0.21	0.36	0.15	0.33	0.10	0.09	0.36
20	0.07	0.05	0.16	0.31	0.12	0.32	0.06	0.08	0.35

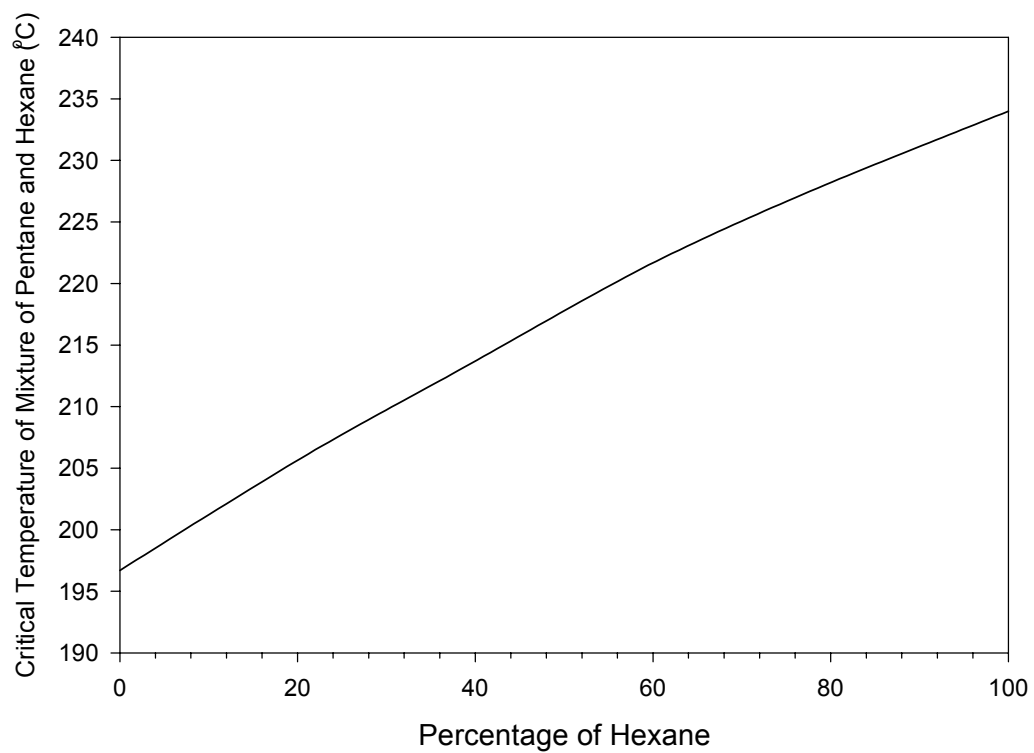


Figure 1. Critical temperature of pentane and hexane mixture with increasing hexane percentage.

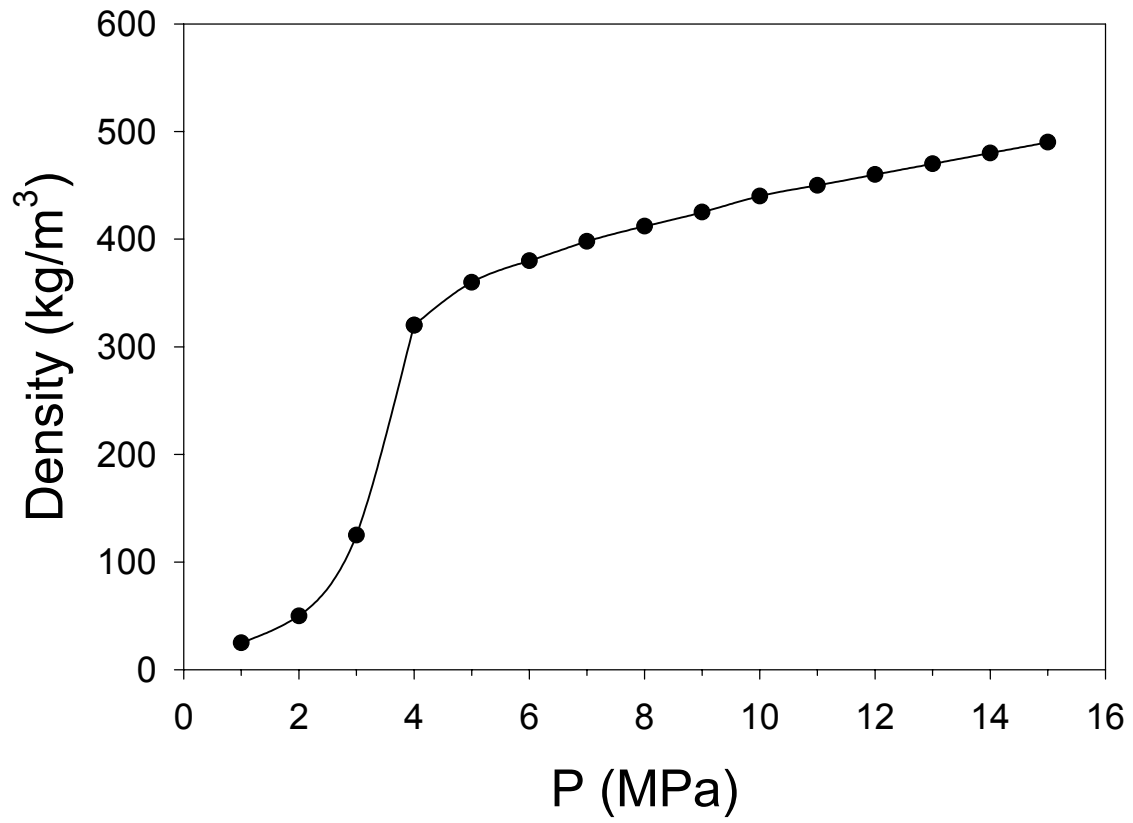


Figure 2: Density versus pressure of the mixture of 55% hexane and 45% pentane.

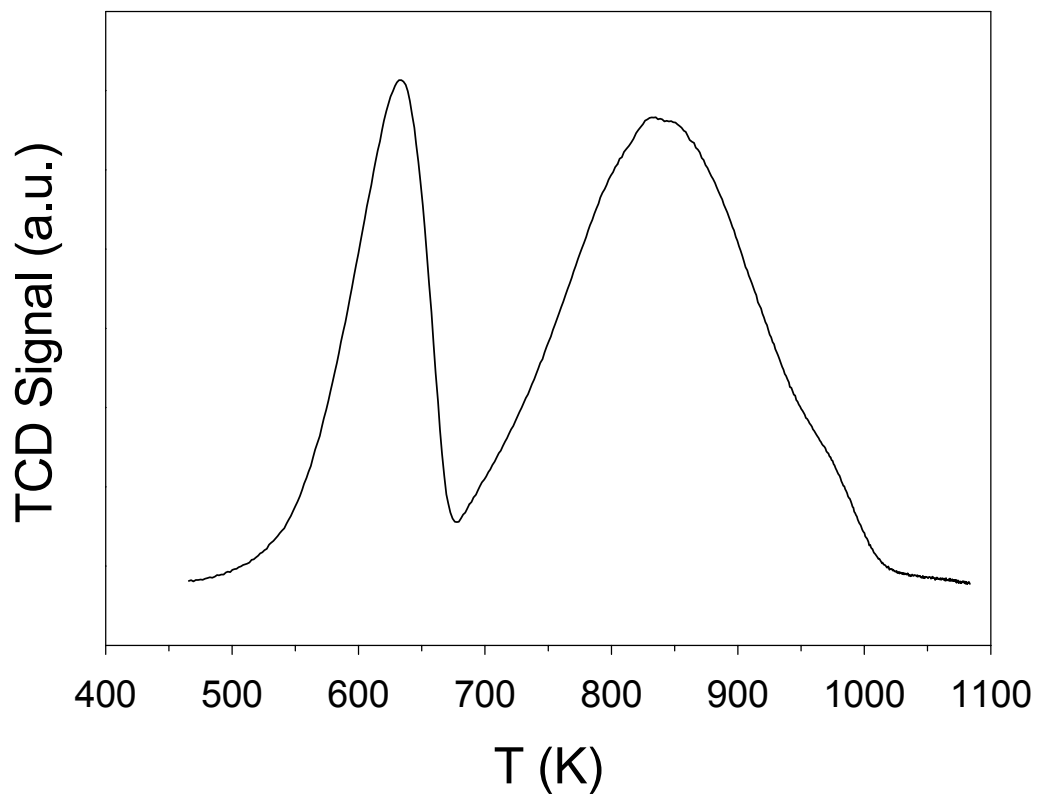


Figure 3: TPR profile of the 25%Co/Al₂O₃ catalyst prepared by the slurry phase impregnation method.

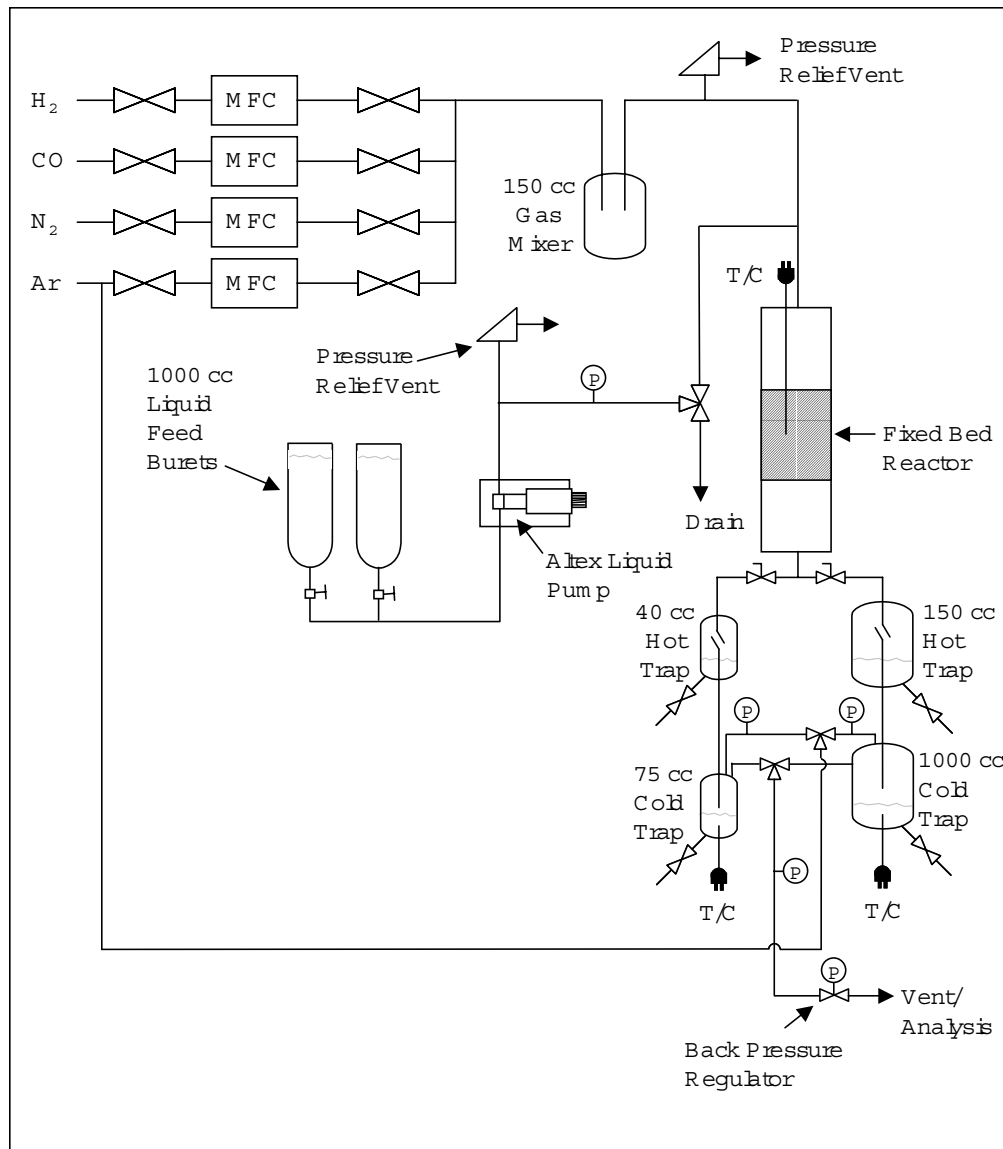


Figure 4: Flow diagram of the supercritical FT reactor system.

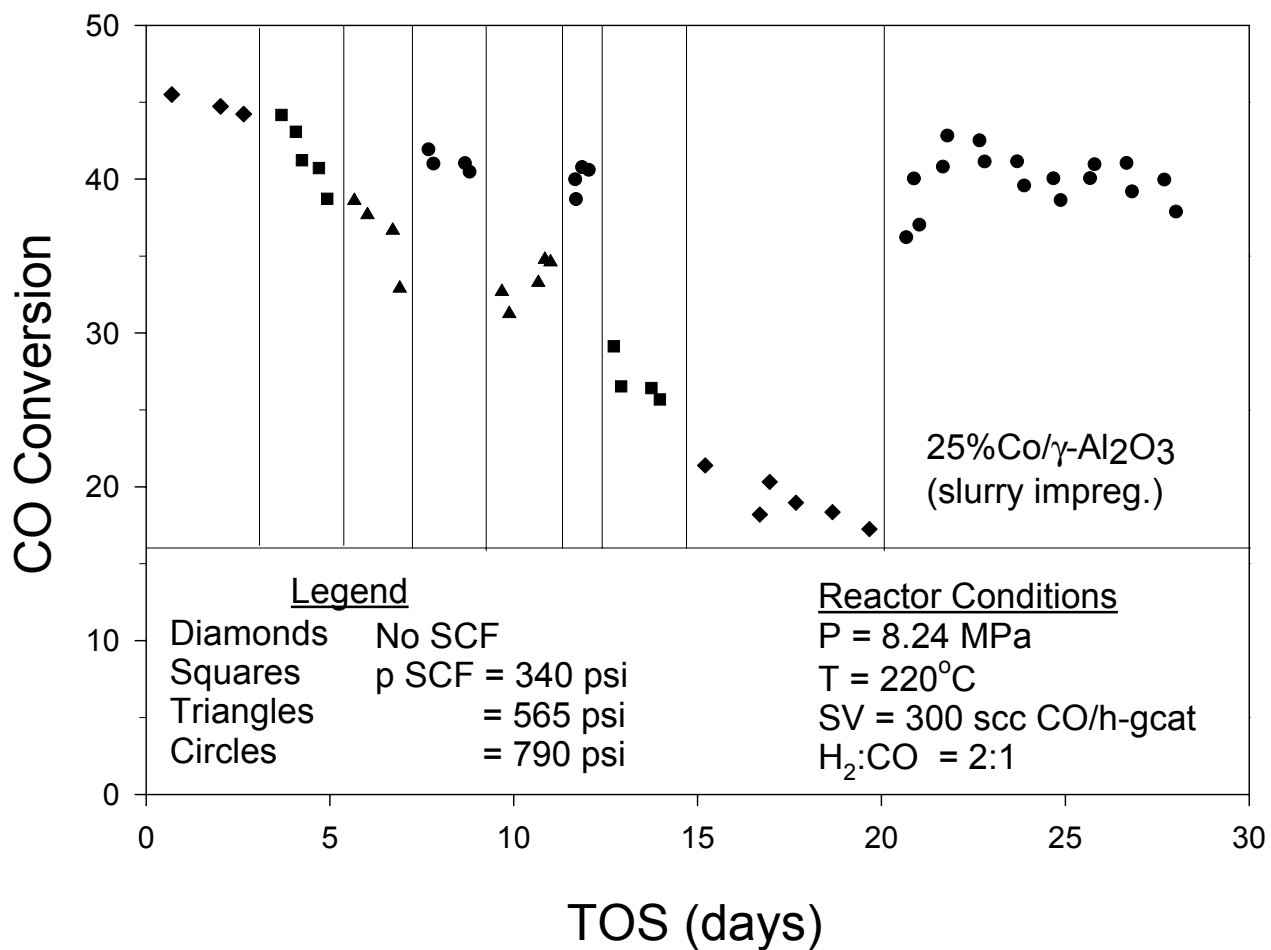


Figure 5: CO conversion vs time-on-stream on a 25%Co/ γ -Al₂O₃ slurry phase impregnation catalyst in a fixed-bed reactor with varying partial pressure of SCF.

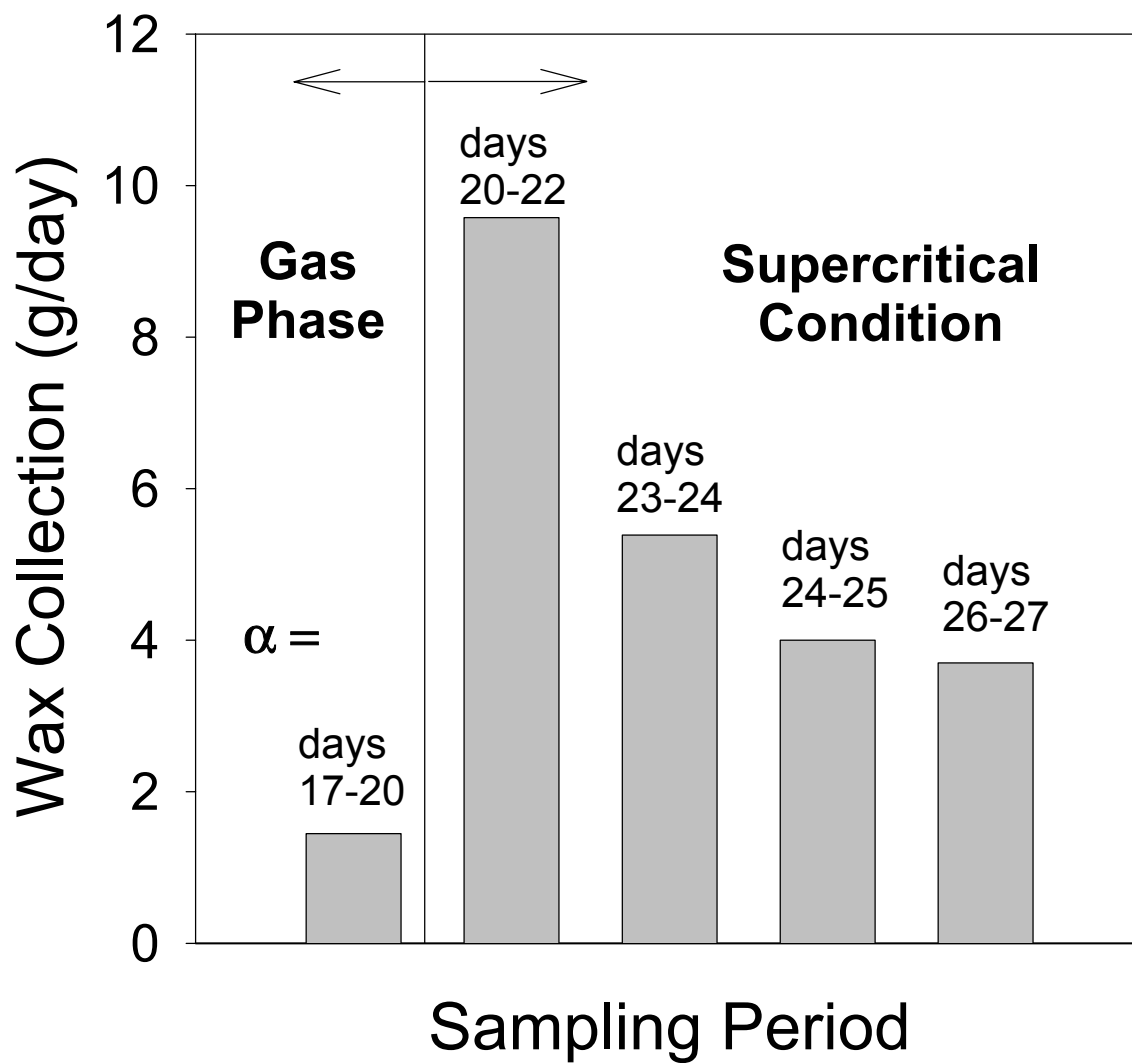


Figure 6: Wax collection during each sampling period.

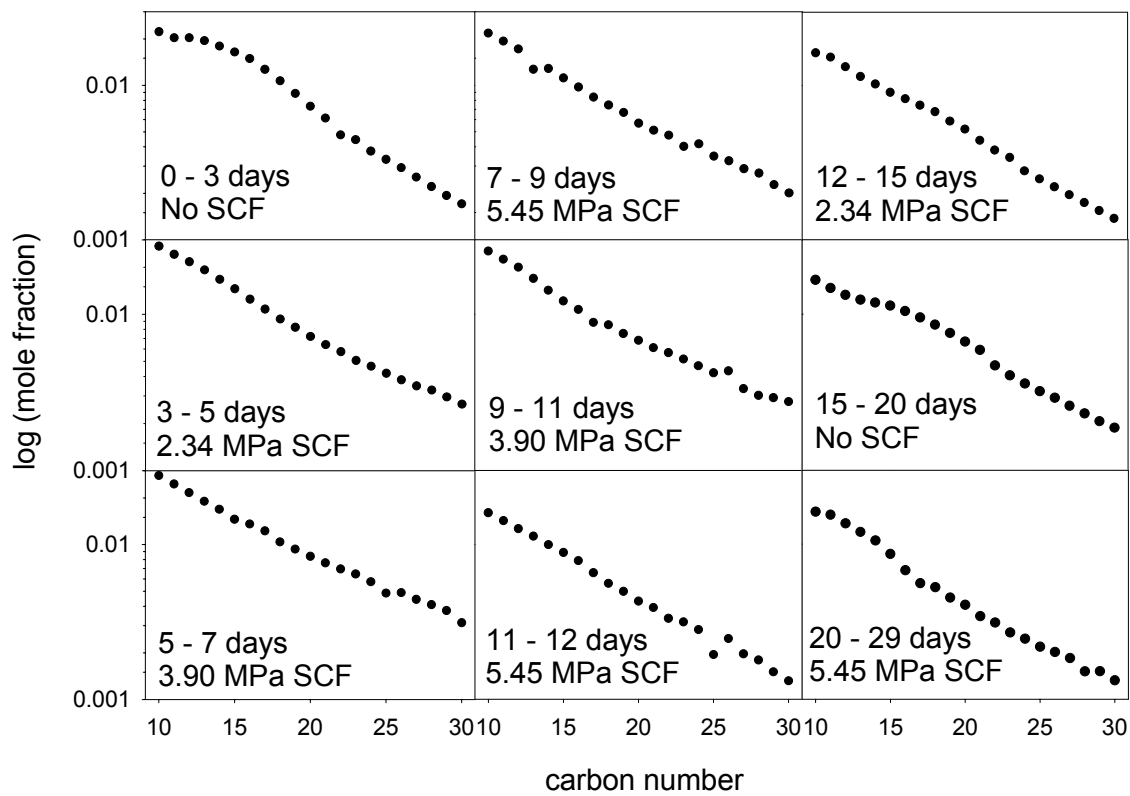


Figure 7: Wax product distribution under nonsupercritical conditions.

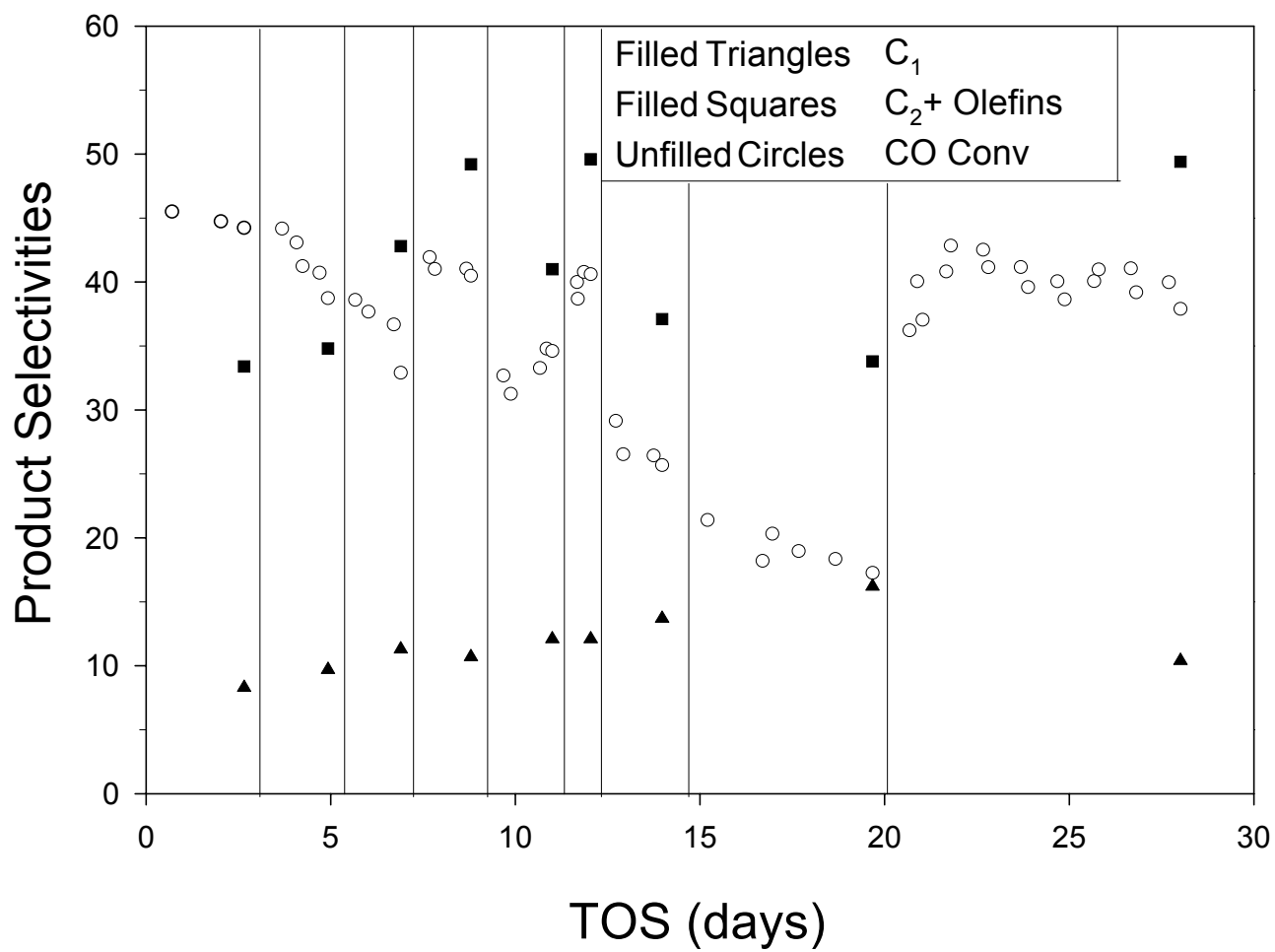


Figure 8: Product selectivities versus time-on-stream.

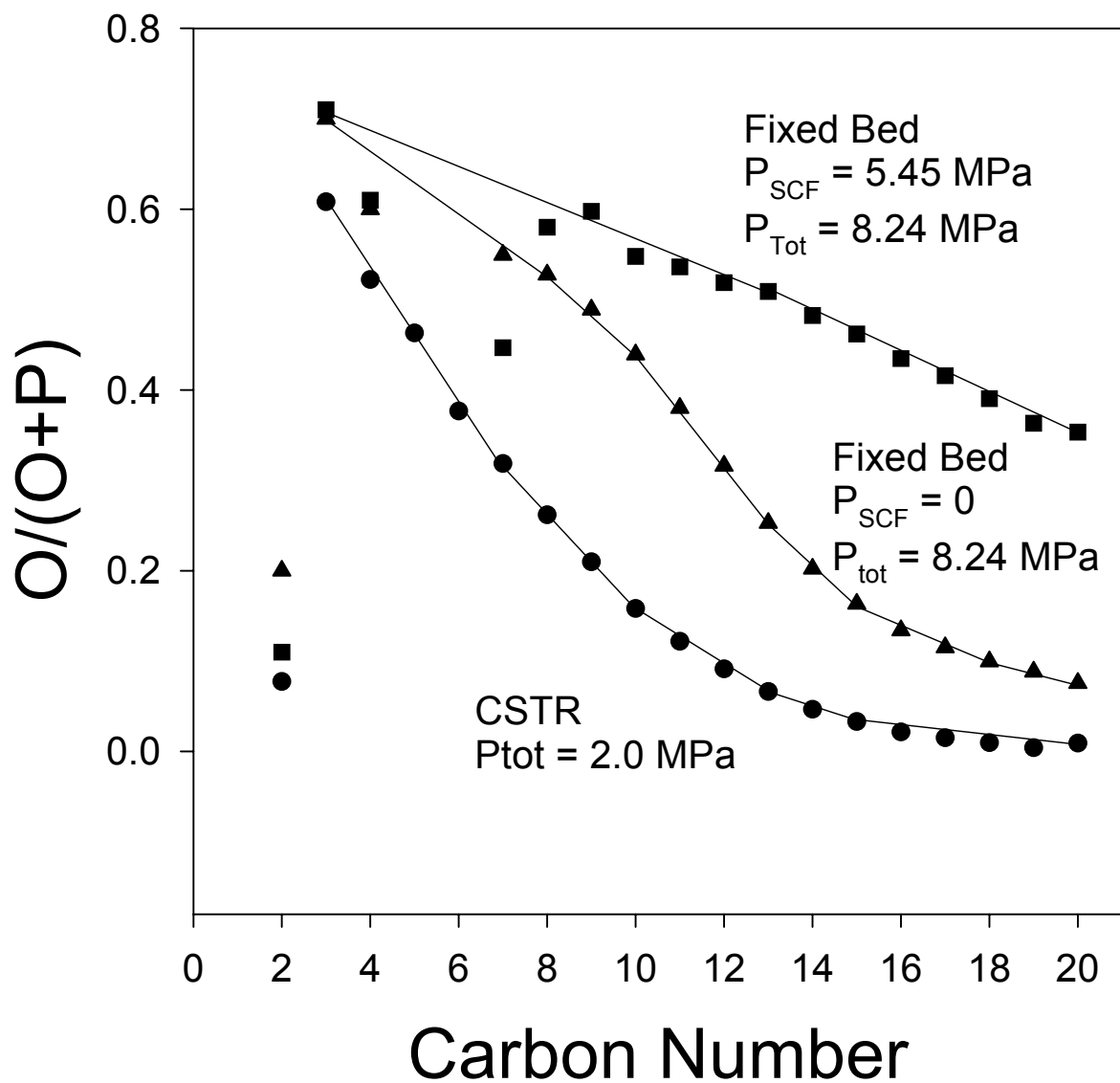


Figure 9: Olefin selectivity as a function of carbon number for supercritical and gas phase FTS.

Task 9. Cobalt Catalyst Life Testing

The objective of this task is to obtain life data on baseline cobalt Fischer-Tropsch catalysts.

No scheduled for further activity to report.

Task 10. Cobalt Catalyst Mechanism Study

The objective of this task is to determine the impact of secondary reactions on the relationship of cobalt Fischer-Tropsch catalysts under conditions appropriate to slurry bubble column reactors.

Task 11. University of California, Berkeley (Subcontract)

The objective of this task is the characterization of the structure and function of active sites involved in the synthesis of high molecular weight hydrocarbons from CO and H₂ on multi-component catalysts based on Fe as the active component.

Our funding has been exhausted as of end of October 2001 and activities for the project have focused on the preparation of the final technical report. The principal investigator is carrying out final revisions and the final report should be finished by mid-February 2002.

Task 12. Reporting/Project Management

Three monthly and one quarterly reports have been completed.